Breaking tolerance to the natural human liver autoantigen cytochrome P450 2D6 by virus infection

Martin Holdener,[1] Edith Hintermann,[1] Monika Bayer,[1] Antje Rhode,[3] Evelyn Rodrigo,[3] Gudrun Hintereder,[2] Eric F. Johnson,[4] Frank J. Gonzalez,[5] Josef Pfeilschifter,[1] Michael P. Manns,[6] Matthias von G. Herrath,[3] and Urs Christen[1]

[1]Pharmazentrum Frankfurt/Zentrum für Arzneimittelforschung, Entwicklung und Sicherheit and [2]Zentrallabor, Johann Wolfgang Goethe University, 60590 Frankfurt am Main, Germany
[3]La Jolla Institute for Allergy and Immunology, La Jolla, CA 92037
[4]The Scripps Research Institute, La Jolla, CA 92037
[5]National Cancer Institute, National Institutes of Health, Bethesda, MD 20892
[6]Medizinische Hochschule Hannover, 30623 Hannover, Germany

Autoimmune liver diseases, such as autoimmune hepatitis (AIH) and primary biliary cirrhosis, often have severe consequences for the patient. Because of a lack of appropriate animal models, not much is known about their potential viral etiology. Infection by liver-tropic viruses is one possibility for the breakdown of self-tolerance. Therefore, we infected mice with adenovirus Ad5 expressing human cytochrome P450 2D6 (Ad-2D6). Ad-2D6–infected mice developed persistent autoimmune liver disease, apparent by cellular infiltration, hepatic fibrosis, "fused" liver lobules, and necrosis. Similar to type 2 AIH patients, Ad-2D6–infected mice generated type 1 liver kidney microsomal–like antibodies recognizing the immunodominant epitope WDPAQPPRD of cytochrome P450 2D6 (CYP2D6). Interestingly, Ad-2D6–infected wild-type FVB/N mice displayed exacerbated liver damage when compared with transgenic mice expressing the identical human CYP2D6 protein in the liver, indicating the presence of a stronger immunological tolerance in CYP2D6 mice. We demonstrate for the first time that infection with a virus expressing a natural human autoantigen breaks tolerance, resulting in a chronic form of severe, autoimmune liver damage. Our novel model system should be instrumental for studying mechanisms involved in the initiation, propagation, and precipitation of virus-induced autoimmune liver diseases.

CORRESPONDENCE
Urs Christen:
christen@med.uni-frankfurt.de

Abbreviations used: Ad-2D6, adenovirus Ad5 expressing human cytochrome P450 2D6; Ad-GFP, adenovirus Ad5 expressing GFP; AIH, autoimmune hepatitis; ALT, alanine aminotransferase; AP, alkaline phosphatase; AST, aspartate aminotransferase; CYP2D6, cytochrome P450 2D6; GGT, γ glutamyl transpeptidase; HCV, hepatitis C virus; ICP4, infected cell protein 4; LDS, liver damage score; LKM-1, type 1 liver kidney microsomal antibody; PBC, primary biliary cirrhosis.

In contrast to other organs, the liver appears more resistant to autoimmune damage caused by local mechanisms of tolerance induction via T cell deletion, inactivation, and apoptosis (1–4). Nevertheless, autoimmune liver diseases comprising a variety of immune-mediated disorders, such as primary biliary cirrhosis (PBC), primary sclerosing cholangitis, and autoimmune hepatitis (AIH), do exist and often cause severe long-term consequences. The resulting syndromes partially overlap, and clinical signs and symptoms are often inconsistent and variable, making a definite diagnosis sometimes difficult (5–7). Infections are prime candidates for initiating autoimmunity in genetically predisposed individuals because they frequently induce strong inflammatory responses in various organs and can attract a multitude of potentially autoaggressive lymphocytes to the site of infection (8). To evaluate whether virus infections can break tolerance to liver autoantigens, we infected mice with adenovirus Ad5 expressing human cytochrome P450 2D6 (Ad-2D6), which constitutes the major human autoantigen in type 2 AIH (AIH-2) (9, 10). Cytochrome P450 2D6 (CYP2D6) is recognized by type 1 liver kidney microsomal antibodies (LKM-1s), which are present in up to 10% of chronic hepatitis C virus (HCV)–infected patients (11) and are the hallmark defining AIH-2 patients (6, 7).

One possible mechanism by which viruses could induce autoimmunity is a structural similarity of virus and host components, a phenomenon commonly referred to as "molecular

M. Holdener and E. Hintermann contributed equally to this work.

The Rockefeller University Press $30.00
J. Exp. Med. Vol. 205 No. 6 1409-1422 www.jem.org/cgi/doi/10.1084/jem.20071859

mimicry" (12). It has been demonstrated in the past that molecular mimicry may be involved in the induction, acceleration, and prevention of autoimmune processes (13–17). Interestingly, the occurrence of LKM-1s in chronic HCV–infected patients might be explained by molecular mimicry, because antibodies recognizing the HCV proteins NS3 and NS5a recognize a specific conformational epitope on CYP2D6 between aa 254 and 288 (18). Furthermore, HCV has the potential to induce autoreactive CD8 T cells, which cross react with the cytochrome P450 isoforms 2A6 and 2A7 that contain sequence homology to HCV aa 178–187 (19). Indeed, antibodies to CYP2A6 have been found in HCV-infected patients (20). Importantly, LKM-1s of AIH-2 patients recognizing CYP2D6 aa 193–212 have been demonstrated to cross react with epitopes of HCV (RNA-dependent DNA polymerase NS5 aa 2977–2996) and CMV (alkaline exonuclease aa 121–140) (21). A further sequence homology has been reported between the immunodominant CYP2D6 epitope, DPAQPPRD, and the infected cell protein 4 (ICP4) of HSV-1 (22). However, definite proof for environmental factors, such as viruses, as inducers of human autoimmune liver disease has been elusive.

Thus, we wished to test, as a proof of principle, whether viral inflammation caused by liver-tropic adenovirus can facilitate the breaking of tolerance to a naturally occurring autoantigen in the liver. This concept has been previously shown in several diabetes models in which virally meditated inflammation provided a "fertile field" for autoimmune reactions, for example the RIP-LCMV mouse (8, 23) and Ins-HA mouse (24). For the present study, we have chosen the human autoantigen CYP2D6 as a target antigen. We generated Ad-2D6 and infected nontransgenic FVB/N and transgenic CYP2D6 mice, expressing human CYP2D6 under the control of its own promoter as a self-antigen in the liver (25). The use of such an Ad-2D6 vector system ensured both a high expression rate of the triggering antigen (CYP2D6) in the liver (antigen-specific initiation) and a potent activation of the immune system by viral infection. We found that infection with Ad-2D6 results in two distinct phases of liver damage: an acute, antiviral phase, characterized by transient elevation of serum aminotransferase levels and minor cellular infiltrations, followed by an autoimmune phase characterized by massive hepatocellular damage, strong cellular infiltration, formation of high titer anti-CYP2D6 antibodies, and extensive hepatic fibrosis.

RESULTS

Infection of mice with adenovirus results in transient hepatic damage

Transgenic CYP2D6 mice and nontransgenic FVB/N littermates were infected with 2×10^{10} particles of adenovirus Ad5 expressing GFP (Ad-GFP), the liver was removed at different days after infection, and expression of GFP was examined under a fluorescence microscope (Fig. 1 A). GFP-expressing cells were detected from day 1 after infection and reached a maximal number at day 7 after infection, when GFP expression was detected throughout the liver. At day 14 after infection, only very few cells were still expressing GFP (Fig. 1 A). Similar expression kinetics for GFP were detected in Ad-GFP–infected wild-type FVB/N mice (not depicted). Upon infection of FVB/N and CYP2D6 mice with either Ad-2D6 or Ad-GFP, all mice developed transient hepatic damage characterized by an elevation of alanine aminotransferase (ALT) and aspartate aminotransferase (AST) serum levels (Fig. 1 B). Values reached up to 150 and 250 U/liter of serum for AST and ALT, respectively, from weeks 1 to 5 after infection. The serum aminotransferase regressed to normal, preinfection levels around week 6 after Ad-2D6 or Ad-GFP infection (Fig. 1 B). Statistical evaluation of the augmentation over time after infection revealed that there was no significant difference between mice that have been infected with Ad-2D6 and Ad-GFP and between FVB/N and CYP2D6 mice (Fig. 1 B). There is, however, a nonsignificant tendency toward an earlier increase in both AST and ALT in mice that have been infected with Ad-2D6. Further, we measured alkaline phosphatase (AP) as a cholestasis marker and found a minor increase at weeks 1 and 2 after infection with Ad-2D6 but not with Ad-GFP (Fig. 1 C). As observed for AST and ALT, this elevation was only transient and no significant increase in AP levels was found at week 4 or later, indicating that no persistent biliary obstruction or cholangitis occurred after infection of mice with either Ad-2D6 or Ad-GFP. No acute or persistent elevation of γ glutamyl transpeptidase (GGT) levels was detected in infected FVB/N and CYP2D6 mice (not depicted). In summary, these data indicate that adenovirus infection by itself results in acute but transient hepatocellular damage.

Infection with Ad-2D6 results in severe and persistent liver damage

To assess the potential for virally triggered autoimmune–mediated liver damage, both humanized CYP2D6 mice and FVB/N littermates were infected with 2×10^{10} particles of Ad-2D6 (or Ad-GFP), and livers were removed at several times after infection. In contrast to the infection of mice with Ad-GFP, Ad-2D6 infection resulted in severe and persistent liver damage. Morphologically, livers of Ad-2D6–infected mice showed several features characteristic for liver damage associated with autoimmune-mediated liver disease and/or chronic viral hepatitis, such as fused liver lobes, hyperplasic nodules, and capsular fibrosis (Fig. 2 A). Importantly, none of these morphological changes occurred in Ad-GFP–infected mice. To semiquantitatively evaluate the morphological appearance, we defined a liver damage score (LDS; Fig. 2 B). LDS was determined over a period of 45 wk for both CYP2D6 and FVB/N mice infected with either Ad-2D6 or Ad-GFP (Fig. 2 C). Interestingly, >50% of wild-type mice already developed the first morphological signs of liver damage at week 1 after infection with Ad-2D6, whereas mice expressing CYP2D6 showed obvious signs of liver damage only at week 2 after Ad-2D6 infection (Fig. 2 C, left). However, no significant difference in the overall LDS between transgenic and wild-type mice was detected at later times (Fig. 2 C, left). Importantly, LDS was persistently elevated in both CYP2D6

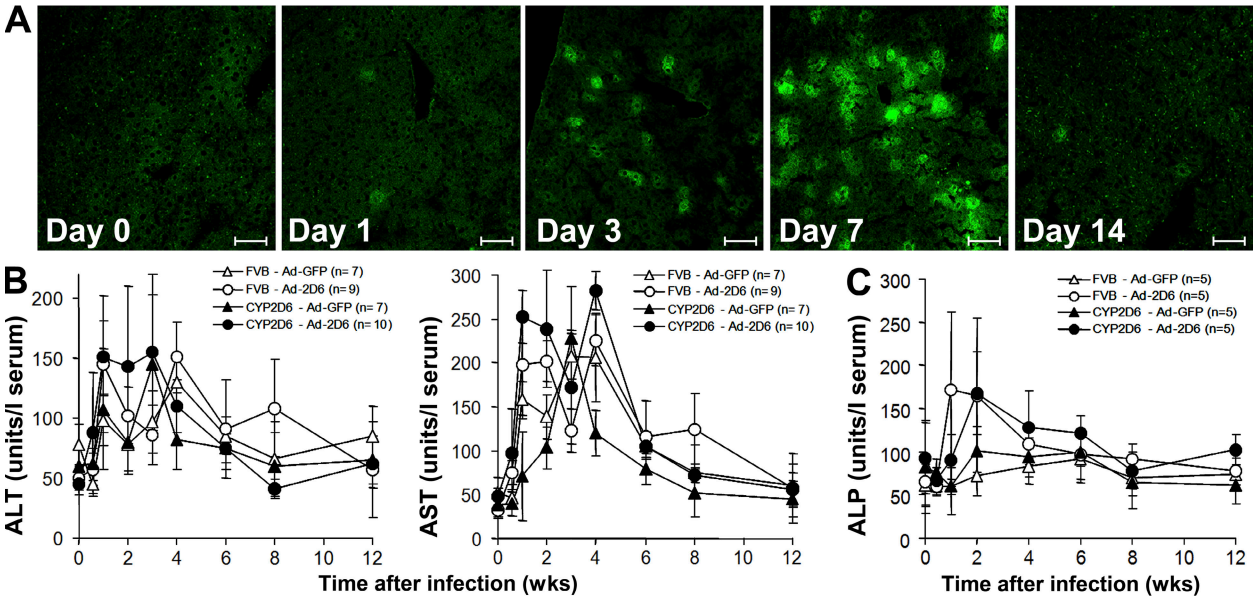

Figure 1. Phase 1: acute liver damage by adenovirus infection. (A) Expression of GFP in liver sections at several times after infection of CYP2D6 mice with Ad-GFP. Bars, 50 µm. (B) Serum levels of ALT and AST in humanized CYP2D6 and wild-type FVB/N mice infected with Ad-2D6 or Ad-GFP at several times after infection. Note that elevations in serum ALT and AST were transient and not persistent. Statistical evaluation (*t* test) revealed no significant differences in AST and ALT augmentation curves over time between Ad-2D6– and Ad-GFP–infected mice (FVB, P = 0.7 [ALT] and 0.79 [AST]; CYP2D6, P = 0.5 [ALT] and 0.13 [AST]) and between FVB/N and CYP2D6 mice (Ad-2D6, P = 0.64 [ALT] and 0.59 [AST]; Ad-GFP, P = 0.31 [ALT] and 0.82 [AST]). (C) Serum levels of AP in humanized CYP2D6 and wild-type FVB/N mice infected with Ad-2D6 or Ad-GFP at several times after infection (n = 5 per group). Transient AP elevation was detected in CYP2D6 and FVB/N mice at weeks 1 and 2 after infection with Ad-2D6 but not Ad-GFP. Statistical evaluation (*t* test) revealed significant differences in serum AP compared with preinfection levels (week 1, P = 0.035 [FVB/N Ad-2D6]; week 2, P = 0.044 [FVB/N Ad-2D6] 0.029 [CYP2D6 Ad-2D6]) and between Ad-2D6– and Ad-GFP–infected mice (week 1, P = 0.03 [FVB] and 0.063 [CYP2D6]; week 2, P = 0.055 [FVB] and 0.029 [CYP2D6]). Data are mean ± SD.

and FVB/N mice even at times later than 3 mo after infection (Fig. 2 C, left). Note that with some minor exceptions, no morphological signs of liver damage were detected in mice infected with Ad-GFP (Fig. 2 C, right). However, statistical evaluation revealed that the LDS was significantly different between Ad-2D6– and Ad-GFP–infected CYP2D6 as well as FVB/N mice ($P < 0.05$ using the Mann-Whitney test). These data demonstrate that although only a transient elevation of ALT, AST, and AP was detected after adenovirus infection of CYP2D6 or FVB/N mice, the viral expression of CYP2D6 resulted in persistent liver damage.

Ad-2D6–infected mice show massive infiltration and fibrosis

Histological examination of liver sections at various times after infection of CYP2D6 and FVB/N mice with either Ad-2D6 or Ad-GFP revealed an early inflammatory phenotype induced by both Ad-2D6 and Ad-GFP (Fig. 3 A, top row). This initial inflammation is likely caused by the direct antiviral immune response mounted to eliminate the infectious agent. However, later on the immunopathology differed between Ad-2D6– and Ad-GFP (control)–infected animals. At week 4, the areas of focal necrosis were becoming larger and increased in number in Ad-2D6–treated mice, whereas Ad-GFP–infected mice showed a reduction of focal necrosis in both size and number (Fig. 3 A, middle row), and at week 8 nearly no focal points of lymphocyte accumulation were detectable in Ad-GFP–treated mice, leaving behind only some scattered lymphocytes (Fig. 3 A, bottom row, far left). In contrast, Ad-2D6–infected mice had a massive increase in inflammation and liver cell destruction at week 8. Interface hepatitis with extensive infiltrates in the periportal and parenchymal regions could be detected, and areas of focal necrosis were growing larger and confluent (Fig. 3 A, bottom row). Semiquantitative analysis of the obtained cellular infiltration data revealed a significant persistence in CYP2D6 and FVB/N mice at week 8 after Ad-2D6 infection when compared with Ad-GFP–infected mice (Fig. 3 B). In FVB/N mice, a significant difference was even found starting from week 4 after infection, suggesting an accelerated liver damage in wild-type mice (Fig. 3 B). Immunohistochemical analysis 2 wk after infection revealed that the cellular infiltrates consisted predominantly of B cells ($B220^+$ cells), CD4 T cells, and macrophages ($F4/80^+$ cells; Fig. 3 C). In contrast, only a few CD8 T cells were found (Fig. 3 C). In support of our initial observation (Fig. 2), we found that FVB/N mice had more rapid cellular infiltration compared with transgenic CYP2D6 mice (Fig. 3 C). Liver sections of Ad-2D6–infected FVB/N mice already displayed a degree of cellular infiltration similar to that observed in CYP2D6 livers at weeks 4

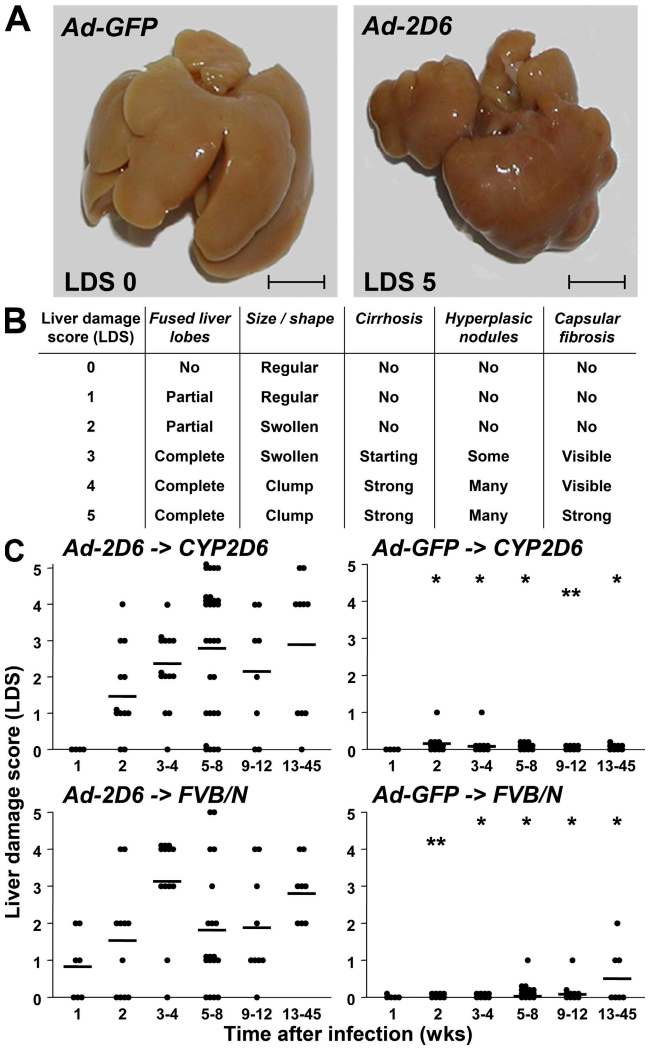

Figure 2. Phase 2: persistent liver damage after infection of mice by Ad-2D6. (A) Paraformaldehyde-fixed livers of CYP2D6 mice infected with either Ad-2D6 or Ad-GFP at week 8 after infection. Bars, 0.5 cm. (B) LDS for evaluation of the morphological appearance of mouse liver after adenovirus infection. Pictures of representative livers of LDS 0 (Ad-GFP infected) and LDS 5 (Ad-2D6 infected) are shown in A. (C) Livers of CYP2D6 and FVB/N mice infected with either Ad-2D6 or Ad-GFP were harvested at several times after infection, and LDS was determined by morphological examination. The mean LDS for each group is indicated by horizontal lines. Note that Ad-2D6–infected mice only develop persistent liver damage. Statistical analysis (Mann-Whitney test) revealed significant differences between Ad-2D6 and Ad-GFP mice at the indicated times. *, $P < 0.01$; **, $P < 0.05$.

and 8 after infection at week 2 after infection, whereas the livers of CYP2D6 mice showed only minor infiltrates at week 2 after Ad-2D6 infection (Fig. 3 C). Liver fibrosis was detected exclusively in Ad-2D6–infected mice, as demonstrated by Sirius red staining of collagen fibers (Fig. 4 A) and immunohistochemistry using an FITC-conjugated anti–collagen I antibody (Fig. 4 B). Sirius red staining was performed with liver sections of CYP2D6 and FVB/N mice obtained at various times after infection with either Ad-2D6 or Ad-GFP. Tissue sections covering the entire liver from three to five mice per experimental group have been analyzed, and a representative picture is displayed for each time point (Fig. 4 A). An increase in subcapsular fibrosis over time was found in Ad-2D6–infected Ad-2D6 and FVB/N mice only (Fig. 4 A), whereas no difference was found in Ad-GFP–infected mice (Fig. 4 A). Interestingly, the development of subcapsular fibrosis was accelerated and more pronounced in wild-type FVB/N mice (Fig. 4 A). For a better visualization of the predominantly subcapsular and interlobular fibrosis, we performed a reconstruction of an immunofluorescent staining of a representative liver section of a CYP2D6 mouse at week 8 after Ad-2D6 infection, covering the entire organ (Fig. 4 B). The figure shows the massive subcapsular fibrosis and the interlobular collagen I deposits that "glue" the individual lobes (including the left and right medial as well as the left lateral lobes) together. No significant collagen I deposits were found in Ad-GFP–infected mice (Fig. 4 B, inset). Costaining for $B220^+$ cells demonstrates that many cellular infiltrates are located in close proximity to the subcapsular collagen I deposits (Fig. 4 B, regions 1 and 2). Similar results have been obtained for Ad-2D6–infected FVB/N mice (unpublished data). These data indicate that Ad-2D6, in contrast to Ad-GFP, induces a persistent damage of the liver in both CYP2D6 and FVB/N mice. Further, the finding that cellular infiltration is augmented (Fig. 3 B) and development of fibrosis is accelerated (Fig. 4 A) in wild-type FVB/N mice indicates the existence of partial tolerance in CYP2D6 mice.

B cell tolerance to the self-target antigen is broken in CYP2D6 mice

Next, we wanted to evaluate the immunological mechanism responsible for the observed liver damage. We collected blood of CYP2D6 and FVB/N mice infected with 2×10^{10} particles of Ad-2D6 or Ad-GFP at various times after infection and determined the activation state of B cells and the titers of anti-CYP2D6 antibodies. We used either a goat anti–mouse pan-Ig antibody or recombinant human CYP2D6 protein to capture total Ig or anti-CYP2D6 antibodies produced by activated B cells in a B cell ELISPOT assay (Fig. 5 A). No striking differences in the frequency of Ig-producing cells of FVB/N or CYP2D6 mice infected either with Ad-2D6 or Ad-GFP were observed (Fig. 5 B, top). In contrast, B cells secreting specific anti-CYP2D6 antibodies were exclusively generated in Ad-2D6–infected mice (Fig. 5 B, bottom). The highest frequency of anti-CYP2D6 antibody-secreting cells of ~0.01% of all splenocytes was found at week 4 after infection (Fig. 5 B). Interestingly, FVB/N mice generated a higher number of anti-CYP2D6 antibody-secreting cells than CYP2D6 mice (Fig. 5 B). These data were mainly reflected in the titer of anti-CYP2D6 antibodies in the serum. IgM-type anti-CYP2D6 antibodies were found to a similar extent in FVB/N and CYP2D6 mice after infection with Ad-2D6, but not Ad-GFP, and reached a maximum titer of 500–900 between weeks 2 and 4 after infection (Fig. 5 C). In contrast, IgG-type anti-CYP2D6 antibodies reached titers up to

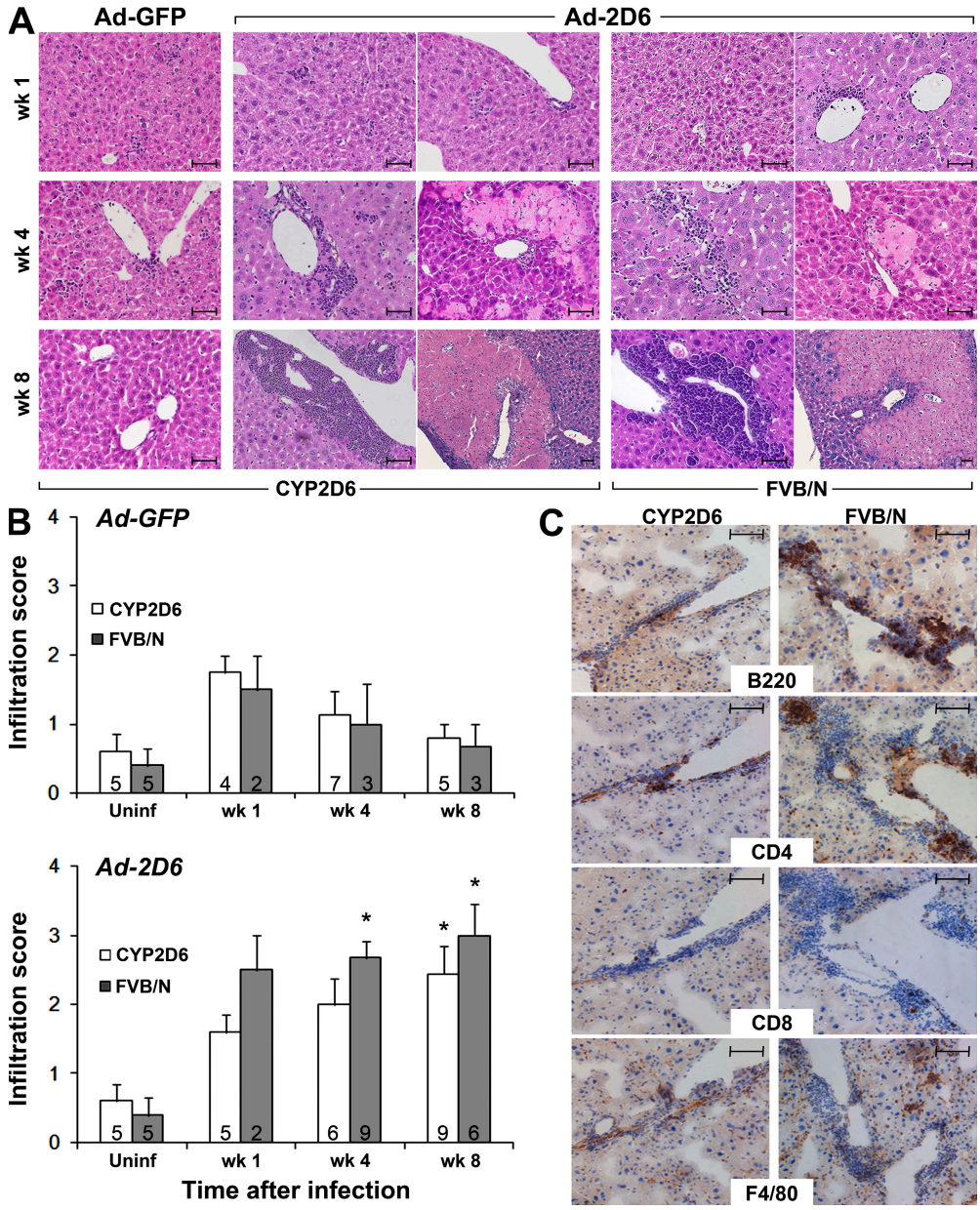

Figure 3. Hepatic necrosis and massive cellular infiltrations after Ad-2D6–infection. (A) Hematoxylin and eosin staining of liver sections obtained from CYP2D6 and FVB/N mice infected with either Ad-2D6 or Ad-GFP at weeks 1, 4, and 8 after infection. Note that persistent hepatic damage (massive cellular infiltrations and significant necrosis) is present in Ad-2D6–infected mice only. Infection of FVB/N mice with Ad-GFP results in a similar histology as Ad-GFP infection of CYP2D6 mice (not depicted). Bars, 50 µm. (B) The following scoring system was used to assess liver infiltration: 0, no visible infiltration; 1, few focal infiltrates; 2, numerous scattered focal infiltrates; 3, few large clusters of infiltrating cells (perivascular or subcapsular); 4, numerous large clusters of infiltrating cells occupying >50% of portal tracts or central veins; and 5, confluent periportal infiltrates. The presented data are mean infiltration scores ± SEM. Statistical analysis (Mann-Whitney test) revealed significant differences between mice infected with Ad-2D6 or Ad-GFP at the indicated times after infection. *, $P < 0.05$. The number of individual mouse livers analyzed per experimental group is indicated at the bottom of each data column. (C) Immunohistochemistry of liver sections of wild-type FVB/N and humanized CYP2D6 mice at week 2 after infection with Ad-2D6. Cellular infiltrations consisted predominantly of B cells (B220), CD4 T cells, and macrophages (F4/80). Bars, 50 µm.

>500,000 in Ad-2D6–infected FVB/N mice and increased with time until around week 6 after infection (Fig. 5 C). We could not detect any CYP2D6-specific IgE-type antibodies in CYP2D6 or FVB/N mice infected with Ad-2D6 or Ad-GFP (unpublished data). The finding that Ad-2D6–infected CYP2D6 mice did not reach as high titers as FVB/N mice (Fig. 5 C) fits well with our previous results (as reported earlier in this paper), in which CYP2D6 mice showed a lower frequency of anti-CYP2D6 antibody-secreting B cells and had attenuated hepatocellular damage and fibrosis compared

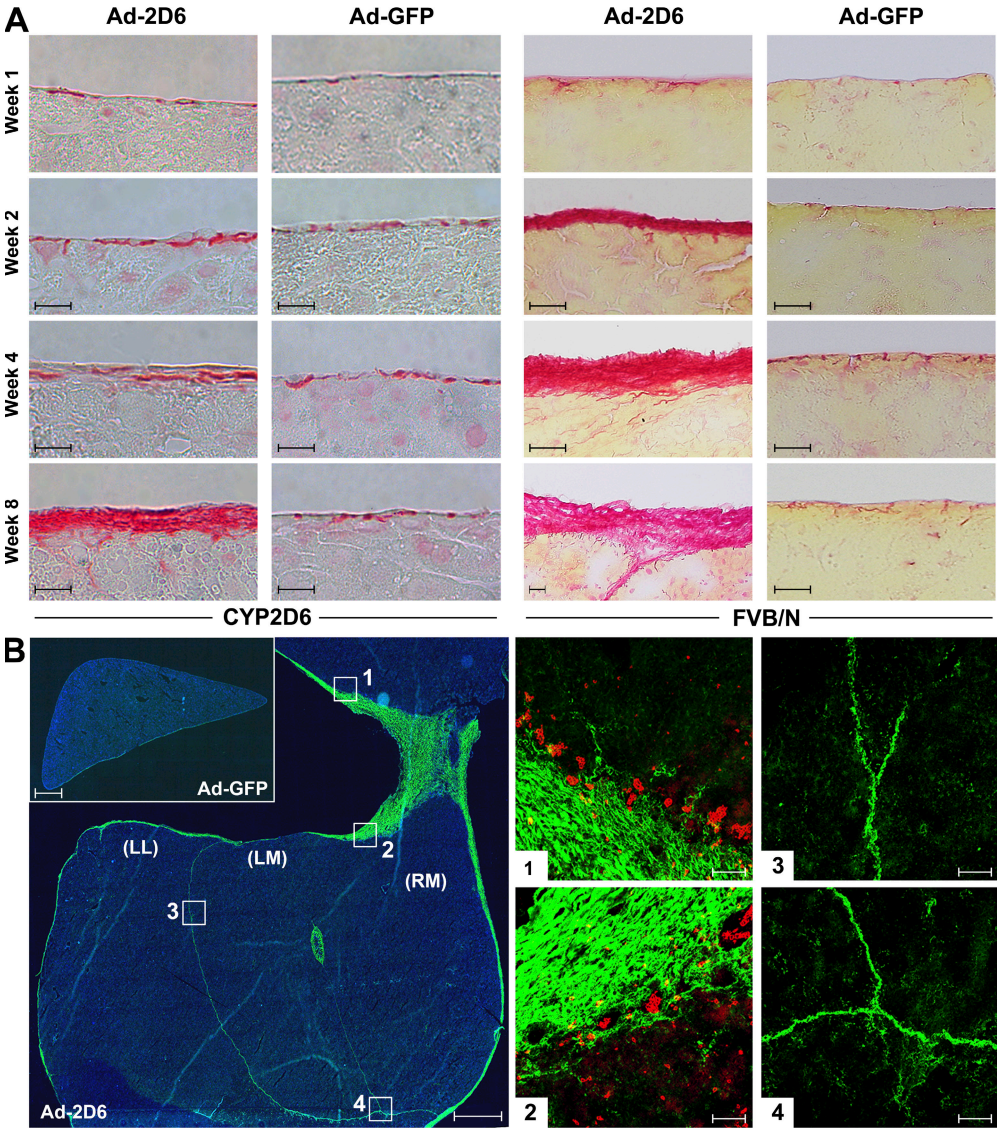

Figure 4. Subcapsular fibrosis after infection of mice with Ad-2D6 but not Ad-GFP. (A) Sirius red staining of collagen fibers in the subcapsular region of the liver at several times after infection of CYP2D6 and FVB/N mice with either Ad-2D6 or Ad-GFP. Tissue sections covering entire livers from three to five mice per experimental group were analyzed, and a representative picture of the subcapsular region is displayed for each time point. Note the increase in magnitude of collagen deposition in Ad-2D6–infected mice over time and the accelerated subcapsular fibrosis in FVB/N compared with CYP2D6 mice. Bars, 20 µm. (B) Reconstruction of a large section of an Ad-2D6–infected CYP2D6 mouse liver (week 8 after infection), including the left medial (LM) and right medial (RM) lobes and the left lateral (LL) lobe, stained for collagen I (green). Note the subcapsular fibrosis and the individual lobes that are glued together by collagen I deposit. (inset) Reconstruction of the left lateral lobe of an Ad-GFP–infected CYP2D6 mouse liver (week 8 after infection). Bars, 0.1 cm. Regions 1–4 are shown at a higher magnification. In addition to staining for collagen I (green), staining for B cells ($B220^+$; red) was overlaid. Regions 1 and 2 show B cells entrapped in pockets within the collagen I deposits in the subcapsular region of the liver. Regions 3 and 4 show areas where two or three individual liver lobes are joined by collagen I fibers. Bars, 50 µm.

with wild-type FVB/N mice. For further characterization, we compared the staining patterns of rat liver sections by the sera of Ad-2D6–infected mice with the sera of patients with various autoimmune liver diseases. A similar LKM-1–like staining pattern was found for the sera from Ad-2D6–infected mice (CYP2D6 and FVB/N mice) and the sera of AIH-2 patients (Fig. 5 D). This pattern was clearly different from the mitochondrial or nuclear staining pattern seen with the sera from patients with PBC (antimitochondrial antibodies) or AIH-1 (antinuclear antibodies [ANAs]), respectively (Fig. 5 D).

Anti-CYP2D6 antibodies in Ad-2D6–infected mice and sera from AIH-2 patients recognize an identical immunodominant epitope

Similar to patients with AIH-2, who generate LKM-1s, Ad-2D6–infected mice generated high titers of anti–human

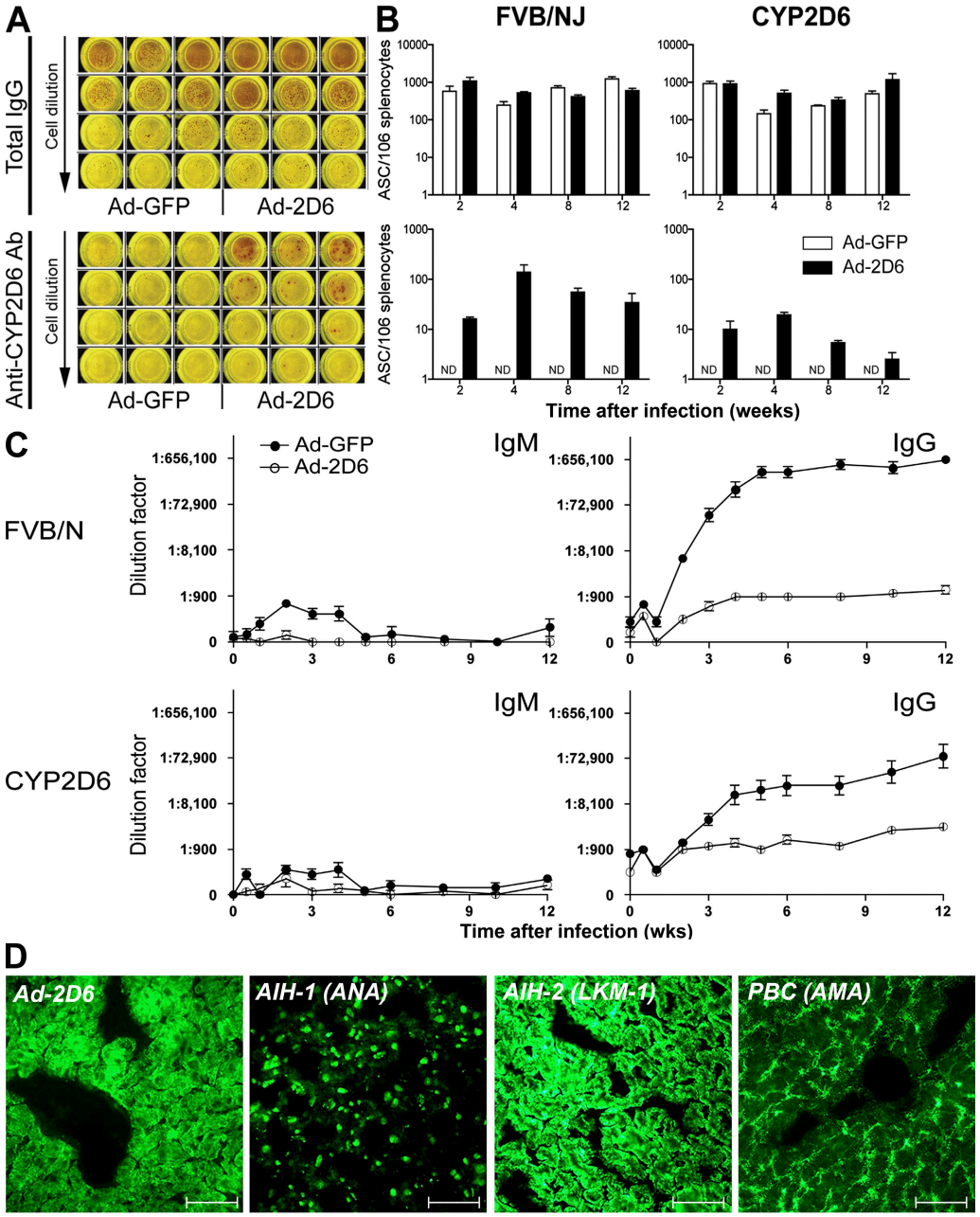

Figure 5. Activation of CYP2D6-specific B cells and generation of anti-CYP2D6 antibodies after Ad-2D6-infection. (A) Pictures of representative end results of total IgG or CYP2D6-specific spot-forming assays. Colored spots indicate the reaction of enzyme-labeled secondary antibodies against secreted IgG and represent one antibody-secreting cell. (B) Quantification of total IgG (top) and CYP2D6-specific IgG (bottom)–secreting cells per 10^6 splenocytes in FVB/N and CYP2D6 mice at the time points indicated. Note that B cells secreting CYP2D6 antibody–specific antibodies were only detectable after Ad-2D6 infection. ND, not detectable. (C) IgM and IgG type anti-CYP2D6 antibody generation in FVB/N and CYP2D6 mice infected with either Ad-2D6 or Ad-GFP over time. Data are mean ± SEM. (D) Representative pictures of rat liver sections stained with sera from Ad-2D6–infected CYP2D6 mice, Ad-2D6–infected FVB/N mice, AIH-1 patients (ANA), AIH-2 patients (LKM-1), and PBC patients (antimitochondrial antibodies), followed by Alexa Fluor 488–conjugated anti–mouse IgG or FITC-conjugated anti–human IgG secondary antibody. Bars, 50 µm.

CYP2D6 antibodies. Thus, we next mapped the dominant human CYP2D6 B cell epitope recognized by the sera of Ad-2D6–infected mice by using the SPOTs technology, in which staggered peptides covering the entire human CYP2D6 sequence are covalently linked to a nylon membrane. Fig. 6 A shows an example of a serum of an Ad-2D6–infected CYP2D6 mouse reacted with the SPOTs membrane. Linear epitopes reacting with the serum are clearly visible and can be easily quantified (Fig. 6 B, top). Interestingly, sera from all Ad-2D6–infected CYP2D6 as well as FVB/N mice predominantly

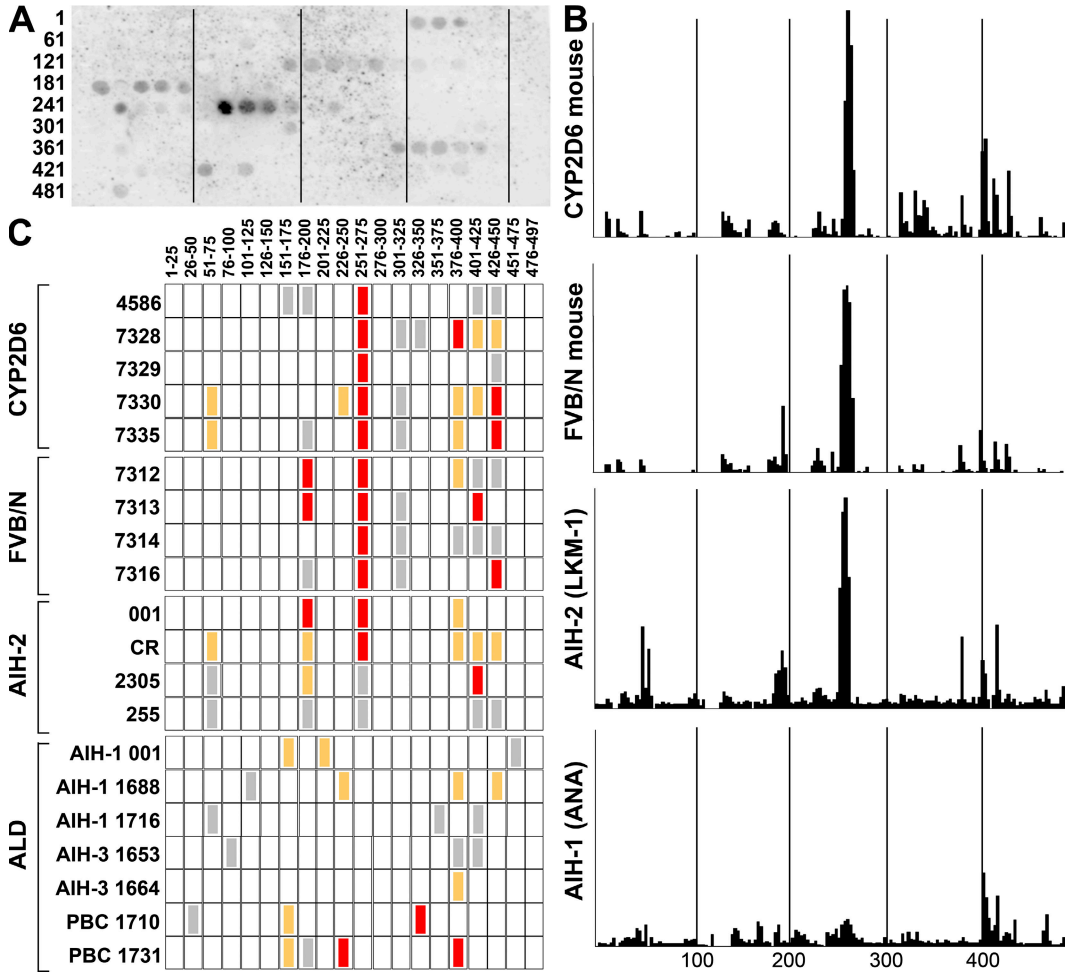

Figure 6. Mouse anti-CYP2D6 antibodies and sera of AIH-2 patients recognize the identical immunodominant CYP2D6 epitope. (A) SPOTs membrane containing staggered peptides of 12 aa in length covering the entire 497 aa of the human CYP2D6 molecule. The membrane was developed with serum of an Ad-2D6–infected CYP2D6 mouse. Numbers indicate the position within the CYP2D6 sequence of the first aa of the first peptide spot in each horizontal lane. (B) Quantification of the serum reactivity profile to SPOTs peptides. Representative serum samples of an Ad-2D6–infected CYP2D6 mouse, an Ad-2D6–infected FVB/N mouse, an AIH-2 patient, and an AIH-1 patient. Numbers indicate the aa position within the human CYP2D6 sequence. (C) For an overview of the epitope profile, the human CYP2D6 sequence was divided into 20 25-aa-long sections, as indicated at the top of each column. Signal intensities of sera from Ad-2D6–infected CYP2D6 and FVB/N mice, patients with AIH-2, and patients with other autoimmune liver diseases, such as AIH-1, AIH-3, or PBC, are indicated in red (strong), orange (medium), gray (low), and white (no reactivity). Note that the region containing the immunodominant WDPAQPPRD epitope (region 251–275) is recognized by all sera of Ad-2D6–infected CYP2D6 and FVB/N mice, as well as by all tested sera of AIH-2 patients, but not by sera from patients with other autoimmune liver diseases.

reacted to a cluster of overlapping peptides within the core aa sequence WDPAQPPRD (CYP2D6 aa 262–270; Fig. 6, B and C). It was previously reported that the majority of LKM-1 sera reacted with a similar region of the CYP2D6 molecule (22, 26–28). Most importantly, in an extensive study with the sera of 26 LKM-1–positive AIH-2 patients, 22 recognized a 33-aa segment of CYP2D6 in this region, and 11 (50%) of these sera recognized the minimal B cell epitope DPAQPPRD (CYP2D6 aa 263–270) (22). Indeed, in our hands four out of four patients with AIH-2 recognized the WDPAQPPRD core sequence (Fig. 6, B [second from bottom] and C). In contrast, sera from patients with other autoimmune liver diseases (AIH-1 and PBC) did not recognize the immunodominant CYP2D6 B cell epitope (Fig. 6, B [bottom] and C). In addition to the immunodominant CYP2D6 aa 262–270 epitope, other epitopes were recognized by FVB/N and CYP2D6 mouse sera as well, although to a much lesser extent and with some variation between individual mice (Fig. 6 C). However, the overall pattern of epitope recognition was mostly overlapping between sera from Ad-2D6–infected mice and patients with AIH-2, but not with the sera of patients with other autoimmune liver diseases (Fig. 6 C).

In summary, our data suggest that the breakdown of B cell tolerance to human CYP2D6 in transgenic CYP2D6 mice induced by infection with adenovirus results in autoimmune reactivity that is very similar to that found in AIH-2 patients.

Importantly, wild-type FVB/N mice, which do not express the human CYP2D6 model antigen but express several mouse Cyp isoenzymes with high homology to human CYP2D6, exhibit even a lesser degree of immunological tolerance toward human CYP2D6 and might therefore generate an even stronger immune response toward human CYP2D6.

DISCUSSION

By infecting CYP2D6 humanized and wild-type FVB/N mice with an adenovirus vector expressing the natural human autoantigen CYP2D6, self-tolerance to CYP2D6 and orthologous mouse cytochrome P450 isoenzymes (Cyp) was broken, resulting in persistent autoimmune liver damage. For the first time, we show the generation of autoantibodies in an animal model with the same specificity as human LKM-1s occurring in AIH-2 patients, combined with severe autoimmune-mediated hepatic damage and characterized by hepatocellular necrosis, massive cellular infiltration, and hepatic fibrosis.

In theory, the liver should be a prime target for autoimmunity. First, because of its function as a detoxifying and drug-metabolizing organ, cellular destruction (i.e., by ethanol) and neoantigen formation (i.e., protein adduct formation by reactive metabolites) can occur. Second, the liver is the target of potential environmental triggering factors for autoimmune disease, including hepatitis, coxsackie virus, HSV, and many more. It has further been suggested that the liver may act as a sink for activated lymphocytes (29, 30). However, the frequencies of autoimmune disorders that specifically afflict the liver, such as AIH (5), PBC (31), or halothane hepatitis (32), are relatively low when compared with other autoimmune diseases, such as type 1 diabetes, certain types of thyroiditis (Hashimoto's disease and Grave's disease), multiple sclerosis, or rheumatoid arthritis. In addition, it is known that liver allografts are less frequently rejected than other transplants (33). Nevertheless, the consequences of autoimmune liver destruction are often severe, including massive hepatic damage, cirrhosis, and subsequent multiorgan dysfunction, which frequently makes liver transplantation unavoidable. Several possible explanations for strong hepatic tolerance have been suggested in the past, including T cell inactivation by antigenic priming in the liver (3), tolerance induction via cross-presentation by liver sinusoidal endothelial cells (1), induction of regulatory T cells by liver sinusoidal endothelial cells (2), and hepatic stellate cell–induced T cell apoptosis (4).

Such immunosuppressive mechanisms certainly have made the generation of a reliable animal model to study persistent autoimmune-mediated liver damage difficult. Although several, mostly transgenic, mouse model systems have been tested in the past, only transient damage to the liver has been detected in most models, such as the HBsAg (34–36), H-2K^b (37), ALB1-LCMV-GP33 (38), LCMV-NP (39), and TF-OVA models (40). In addition, induction of disease often required the transfer of antigen-specific lymphocytes (34–36, 38). In another recent study, AIH-like disease was reported in mice by xenoimmunization using a plasmid containing the antigenic region of CYP2D6 (41). However, only coexpression of CYP2D6 and IL-12 resulted in significant inflammation in the liver. In addition, only minor elevations in serum ALT and a transient generation of low-titer anti-CYP2D6 antibodies with large interindividual differences were stated (41).

A common hypothesis to explain the etiology of autoimmune disease is genetic predisposition of the host (intrinsic risk factors) paired with environmental triggers (8). Many autoimmune diseases have been associated with pathogen infection (for reviews see references 8, 42, 43). To date no firm proof for environmental factors, such as viruses, as inducers or enhancers of most human autoimmune diseases, including human AIH, has been found. Direct evidence for viruses to induce or accelerate autoimmune disease is, however, hard to come by because (a) virus infections are often "hit and run" events that leave no traces behind at the time of diagnosis of autoimmune disease; (b) patients suffering from autoimmune diseases, as well as healthy individuals, undergo several pathogen infections during their lifetime; (c) viruses might not directly induce autoimmune disease but instead accelerate a preexisting autoimmune condition to progress to clinical disease; (d) the exact time, location, and magnitude of infection might be important; and (e) some pathogens have even been demonstrated to have protective properties (44, 45). However, several pathogens have been associated with autoimmune liver disease. For PBC, it has been suggested that the xenobiotic-metabolizing bacterium *Novosphingobium aromaticivorans* might be involved in the initiation of the diseases (46). For AIH, several studies implicate viruses, such as measles virus, hepatitis viruses, CMV, and Epstein-Barr virus, in its initiation (for reviews see 6, 47). In particular, sequence homology has been reported between the immunodominant CYP2D6 epitope DPAQPPRD and ICP4 of HSV-1 (22). Further, a study by Kerkar et al. demonstrates that a considerable fraction of AIH-2 patients (12 out of 13, or 93%) and LKM-1–positive patients with chronic HCV infection (5 of 10, or 50%) carry antibodies reacting to the CYP2D6 epitope RLLDLA (aa 204–209) (21). Interestingly, this reactivity can be neutralized by incubation with epitopes of HCV (RNA-dependent DNA polymerase NS5 aa 2977–2996 containing the core sequence RLLDLS) and CMV (alkaline exonuclease aa 121–140 containing the core sequence RLLDLA), suggesting a possibility of molecular mimicry as a mechanism involved in the etiology of AIH (21).

As a proof of principle of how environmental factors can initiate autoimmune liver disease in an animal model, we used an adenovirus expressing the natural major human liver autoantigen CYP2D6 as a triggering factor. One has to acknowledge that, in this system, large amounts of the target/triggering protein (CYP2D6) are being expressed from the adenoviral vector directly in the liver in context with a significant viral inflammation of the target organ. Thus, our current findings underline the strong need for inflammation to trigger autoimmune liver damage. In our case, a hepatotropic adenovirus was capable of preparing a fertile field (48) for the arrival of autoaggressive lymphocytes. It is remarkable that, under these conditions, strong systemic induction

of CYP2D6-specific B cells was still required, and even the expression of transgenic human CYP2D6 under control of its own promoter in CYP2D6 mice was not sufficient to break tolerance with a virus that did not express CYP2D6 (Ad-GFP control).

The 2D6 isoform of the large cytochrome P450 enzyme family is the major antigen component specifically recognized by LKM-1s (9, 10), which are the defining hallmark autoantibodies present in patients afflicted with AIH-2 (5–7). AIH is a severe form of an adverse immune reaction resulting in the progressive destruction of the hepatic parenchyma (49). Among AIH patients, ~10% are affected by AIH-2 and develop LKM-1s, which are regarded as serological markers for AIH-2. Besides LKM-1, up to 50% of AIH-2 patients develop anti–liver cytosol type 1 antibodies, and ~10% develop LKM-3s to family 1 uridine 5′-diphosphate glucuronosyltransferase (7). However, the majority (90%) of AIH patients are affected by AIH-1 and develop ANAs, anti–smooth muscle actin antibodies, atypical perinuclear antineutrophilic cytoplasmic antibodies, and anti–soluble liver antigen/liver pancreas antigen antibodies, which are all less well characterized than LKM-1s (6, 7). Susceptibility factors for the individual AIH subtypes are dominated by the MHC haplotype, although other factors, such as complement genes, Igs, and TCR variants, may play a minor role as well (6). In contrast to AIH-1, which is predominantly associated with HLA-DR3 and HLA-DR4, AIH-2 is primarily associated with HLA-DRB1 and HLA-DQB1, and the presence of HLA-DR2 seems to be protective (for details see Krawitt [6]). Autoreactive CD4 and CD8 T cells specific for CYP2D6 have been found in the blood and the liver of AIH-2 patients (50, 51). However, although the major target antigens have been characterized on the level of specific epitopes, the etiology of AIH-2 is only poorly understood. It is intriguing that the CYP2D6 antigen performed well as an autoantigenic target in our model of adenovirally induced liver inflammation, underlining its importance in liver autoimmunity across species and under various conditions. Interestingly, our model system exhibited two phases of liver injury after infection of CYP2D6 and FVB/N mice with Ad-2D6. First, infection with adenovirus (Ad-2D6 as well as Ad-GFP) initiated an antiviral immune response associated with transient damage to the liver, characterized by minor elevation of serum aminotransferase levels and focal infiltration by mononuclear cells. It had been previously reported (52) that replication-deficient adenoviruses can induce acute injury and inflammation. As early as 1 h after infection with 10^{10} particles of an adenovirus-βgal vector, expression of chemokines, such as macrophage inflammatory protein 2, monocyte chemoattractant protein 2, and IFN-inducible protein 10, was strongly increased and neutrophils infiltrated immediately thereafter (52). All adenovirus vectors tested by Muruve et al. did cause transient hepatic damage and cellular infiltrates (52) similar to the focal clusters of infiltrating cells we detected at day 7 for Ad-2D6 and Ad-GFP in our own experiments (Fig. 3 A). Our crucial observation in this study, however, is that a second autoimmune phase with persistent hepatic damage follows the viral inflammation, but only when the triggering adenovirus drives the expression of the CYP2D6 autoantigen. Generation of anti-CYP2D6 antibodies at very high titers was restricted to mice infected with Ad-2D6, whereas infection of mice transgenically expressing human CYP2D6 with Ad-GFP was not sufficient for anti-CYP2D6 antibody formation. The specificity of these antibodies was directed to the same immunodominant CYP2D6 epitope that was recognized by LKM-1s found in the sera of AIH-2 patients. These data suggest that the breakdown of tolerance in Ad-2D6–infected mice might be mediated via a similar pathway than in patients suffering from AIH-2. It is further important to note that virus infection was necessary to induce liver disease in the CYP2D6 model system. We injected CYP2D6 and FVB/N mice with recombinant human CYP2D6 in combination with Poly-IC (i.v.), CpG (i.v.), or CFA (s.c.). None of these mice showed any signs of liver damage, such as elevated serum aminotransferases, cellular infiltrations, and fibrosis. In these experiments only s.c. injection of recombinant human CYP2D6 emulsified in CFA resulted in the generation of anti-CYP2D6 antibodies at a titer similar to Ad-2D6–infected mice (unpublished data). These data indicate that the generation of anti-CYP2D6 antibodies per se is not sufficient to induce autoimmune liver damage.

Interestingly, wild-type FVB/N mice showed an accelerated course of hepatic damage with an enhanced number of activated CYP2D6-specific B cells and generated higher titers of anti-CYP2D6 antibodies compared with transgenic CYP2D6 mice, indicating that tolerance to human CYP2D6 is harder to overcome in CYP2D6 mice. Although, none of the mouse cytochrome P450 family genes (*Cyp*) encode an isoenzyme with similar catalytic activity as human CYP2D6 (53), wild-type FVB/N mice do express Cyp isoenzymes with high sequence homology to the human CYP2D6 and other human CYP isoenzymes. A screening of the National Center for Biotechnology Information databank revealed that the mouse Cyp isoenzymes Cyp2D9, Cyp2D11, Cyp2D22, and Cyp2D26 display up to 75% aa sequence homology to human CYP2D6 (available from GenBank/EMBL/DDBJ under accession nos. BAE25635, P24457, AAF34652, Q8CIM7, and M33388, respectively). Further, the mouse Cyp2D26 protein contains an aa sequence (aa 262–270) identical to the human CYP2D6 epitope WDPAQPPRD, which was found to be immunodominant in AIH-2 patients and in Ad-2D6–infected mice. Thus, upon challenging FVB/N mice with Ad-2D6, autoimmune liver damage was most likely induced because of true molecular mimicry between the human CYP2D6 expressed via the adenovirus system and homologous mouse sequences (i.e., mouse Cyp2D26), as demonstrated by our experiments. However, tolerance to human CYP2D6 was more pronounced in CYP2D6 humanized mice, which express the identical human CYP2D6 molecule and exhibited delayed liver damage, a lower frequency of activated B cells, and a lower anti-CYP2D6 antibody titer. These observations allow for the speculation that similar yet not identical

autoantigens might be better targets for autoimmune reactions, because central and peripheral tolerance mechanisms will be less efficient.

We would like to propose that molecular mimicry remains one of the possible mechanisms that could become relevant with a concomitant viral infection of the liver. Indeed, our earlier studies have shown that molecular mimicry can enhance an ongoing autoimmune process (15), although cross-reactivity alone was not able to elicit autoimmune diabetes in naive animals. Indeed, several pathogens confer molecular mimicry with human CYP2D6. Most prominently, ICP4 of HSV-1 carries the peptide sequence PAQPPR, which is also found in the immunodominant human CYP2D6 epitope DPAQPPRD (22). However, no epidemiological association that would link HSV-1 infection with AIH-2 has been reported (22). In contrast, an epidemiological link was demonstrated for HCV infection (54, 55), and antibodies to HCV were found in a large proportion of AIH-2 patients (56, 57). In addition, LKM-1s were detected in up to 10% of HCV-infected individuals, depending on the geographic origin (11). It is, however, noteworthy that LKM-1s of HCV-infected patients recognize a different pattern of CYP2D6 epitopes than LKM-1s of AIH-2 patients (11, 26, 58), indicating a divergent pathway leading to the breakdown of tolerance toward CYP2D6 in HCV-infected individuals. It is therefore important to further analyze the mechanisms of tolerance breakdown to human CYP2D6 in the humanized CYP2D6 mouse, which generates anti-CYP2D6 antibodies recognizing a similar epitope pattern as human LKM-1s, and to analyze the kinetics of epitope recognition by the sera of AIH-2 patients in more detail. It is important to note that the CYP2D6 reactivity of LKM-1s is not restricted to the immunodominant WDPAQPPRD epitope (aa 262–270). The detection of several other CYP2D6 epitopes that have been recognized by various proportions of patients' sera has been reported, including the regions aa 321–351, aa 373–389, and aa 410–429 (26); aa 196–218 (59); aa 193–212, aa 238–257, aa 268–287, and aa 478–497 (21); and aa 284–391, aa 412–429, and the conformational epitopes aa 1–146 (60) and aa 321–379 (58). However, it seems that the outcome of these studies was largely dependent on the assays used and the selection of LKM-1 sera analyzed. It will therefore be important to dissect these immunoreactive epitopes in more detail to screen for pathogen structures conferring molecular mimicry. A very recent article reports a dominant CD8 T cell reactivity to the HLA-A2*0201–restricted CYP2D6 epitope aa 245–254 (61). Interestingly, aa 245–254–specific CD8 T cells could be detected in sections of an explanted liver of an AIH-2 patient by in situ MHC tetramer staining (61). These data indicate that besides the overwhelming B cell/antibody–mediated immune response to liver autoantigens, an aggressive CD8 T cell–mediated process might be involved in the pathogenesis of autoimmune liver diseases such as AIH-2. Thus, it will be important to further develop animal models reflecting all the aspects of the autoreactive immune response. In this context, it is noteworthy that a similar approach of virus-induced inflammation and breakdown of self-tolerance has been used to develop an animal model for myocarditis. Infection of susceptible BALB/c mice with a "heart-passaged" Coxsackie virus B3 containing cardiac myosin caused acute and chronic myocarditis similar to the human disease (62). Interestingly, such mice quickly generated autoantibodies specific for cardiac myosin, suggesting that, similar to our CYP2D6 model, concomitant infection of and antigen delivery to the target organ breaks tolerance and induces disease.

It was the goal of our study to generate an experimental model for virally induced autoimmune liver disease. Infection with an adenovirus expressing human CYP2D6 with 75% sequence homology to mouse Cyp2D isoenzymes elicited persistent damage to the liver associated with anti-CYP2D6 autoantibodies. A first transient phase of liver damage caused by the antiviral response was followed by permanent autoimmune liver damage. Importantly, neither TCR transgenic T cells nor transgenic expression of the autoantigen were required in this model, which brings it much closer to an immunological scenario that one could envision happening in human disease. Thus, our model system serves as a hallmark to further investigate and characterize the immunopathological mechanisms that lead to loss of tolerance to human autoepitopes and such a chronic hepatocellular destruction. Finally, such models may help to establish a basis to evaluate possible treatments for human autoimmune liver diseases.

MATERIALS AND METHODS

Mice and viruses. CYP2D6 humanized mice, generated by microinjection of the entire human *CYP2D6* gene, including its promoter region, into the pronucleus of fertilized FVB/N mouse eggs to produce a transgenic mouse line (25), were provided by F.J. Gonzalez (National Cancer Institute, Bethesda, MD). Wild-type FVB/NHsd mice were purchased from Harlan. Ad-2D6 was created by homologous recombination in *Escherichia coli* BJ5183 between a shuttle vector containing the cDNAs for CYP2D6 and pAdE1^{-}E3^{-} (63). Ad-GFP was a gift from D.J. von Seggern (The Scripps Research Institute, La Jolla, CA). Unless described otherwise, mice were injected with a total of 2×10^{10} particles of Ad-2D6 or Ad-GFP (i.p. and i.v.). All animal experiments were approved by the local Ethics Animal Review Board (Darmstadt, Germany).

Patient sera. All human sera were from the human serum library of the Department of Gastroenterology, Hepatology and Endocrinology of the Medizinische Hochschule Hannover and have been previously tested for antigen specificity (antimitochondrial, liver–kidney microsomal, and smooth muscle and antisoluble antibodies) by standardized immunofluorescence and competitive ELISA procedures (64). All patients have been clinically diagnosed with either type of AIH or PBC. The blood procurement protocol and analysis was approved by the Ethics Committee of the Medizinische Hochschule Hannover.

Serum values for liver damage. ALT and AST were determined by serum aminotransferase enzyme activity assays (BioTron Diagnostics Inc.) using 7.5-μl mouse or human serum. ALT and AST serum levels (U/liter) were calculated using normal and abnormal serum standards (BioTron Diagnostics Inc.). AP and GGT were measured by the central laboratory of the Clinic of the Johann Wolfgang Goethe University. Statistical evaluation of the changes in ALT, AST, GGT, and AP serum levels over time after infection with Ad-GFP or Ad-2D6 was performed by the *t* test using Prism software (version 3.0; GraphPad Software, Inc.). $P < 0.05$ was considered significant.

Immunohistochemistry. Livers were harvested at the times indicated, immersed in Tissue-Tek OCT (Bayer), and quick-frozen on dry ice. 6-μm tissue sections were cut using a cryomicrotome and mounted on sialin-coated slides (Superfrost PLUS; Thermo Fisher Scientific). Sections were fixed with 90% ethanol at −20°C, and after washing in PBS an avidine-biotin blocking step was included (Vector Laboratories). Primary and biotinylated secondary antibodies (Vector Laboratories) were incubated with the sections for 30 min each, and a color reaction was obtained by sequential incubation with avidine-peroxidase conjugate (Vector Laboratories) and diaminobenzidine-hydrogen peroxide. Primary antibodies used were as follows: rat anti–mouse B220, rat anti–mouse CD4, rat anti–mouse CD8α, and rat anti–mouse collagen I (all from BD Biosciences); and rat anti–mouse F4/80 (AbD Serotec). For immunofluorescence stainings, FITC-conjugated rat anti–mouse collagen I and rhodamine X–conjugated rat anti–mouse B220 (both from BD Biosciences) were used. For the staining of rat liver sections, sera of Ad-2D6–infected CYP2D6 and FVB/N mice and patients' sera were diluted in PBS containing 2% FCS (1:250). Alexa Fluor 488–conjugated rabbit anti–mouse (Invitrogen) or FITC-conjugated anti–human IgG (Vector Laboratories) antibodies were used as secondary antibodies at a dilution of 1:200. Sirius red staining was performed using sections of formalin-fixed paraffin-embedded livers. After deparaffinization and rehydration, sections were incubated for 5 h at room temperature in a Sirius red solution containing 0.1% saturated picric acid (Electron Microscopy Sciences). Sections were washed in two changes of 0.01 N HCl for 2 min, rinsed in water, dehydrated in three changes of absolute ethanol for 1 min each, and mounted. Hematoxylin and eosin staining was performed using sections of paraffin-embedded paraformaldehyde-fixed livers by Pacific Pathology Inc. Cellular infiltration into the liver of adenovirus-infected mice was assessed by the following scoring system: 0, no visible infiltration; 1, few focal infiltrates; 2, numerous scattered focal infiltrates; 3, few large clusters of infiltrating cells (perivascular or subcapsular); 4, numerous large clusters of infiltrating cells occupying >50% of portal tracts or central veins; and 5, confluent periportal infiltrates. Infiltrations in tissue sections covering the entire liver were scored in a blinded fashion, and the scoring data were statistically evaluated using the Mann-Whitney test for nonparametric data. $P < 0.05$ were considered significant.

Serum anti-CYP2D6 antibody ELISA. To detect antibodies specific for human CYP2D6, 96-well microtiter plates were coated overnight at 4°C with 0.25 μg/ml of recombinant human CYP2D6 (Invitrogen) in 100-mM of carbonate buffer (pH 9.6), and plates were blocked with 2% FCS in PBS for 90 min at room temperature. Sera were added in PBS containing 2% FCS and were incubated for 90 min at 37°C. The dilution series for each serum started at 1:300, followed by 1:2 dilution steps down to a final dilution of 1:656,100. AP-labeled goat anti–mouse IgM or IgG antibody (1:2,000; SouthernBiotech) was added for 90 min, and the reaction was developed by the addition of ECF substrate (GE Healthcare). Fluorescence intensity was determined using a Storm 560 (GE Healthcare). Sera dilutions with values of three standard deviations above the mean value of negative controls were considered positive.

Detection of antibody-secreting cells. To detect total or CYP2D6-specific antibody-secreting cells, 96-well filter plates (MAHA; Millipore) were coated with 5 μg/ml of goat anti–mouse IgG+IgA+IgM (Invitrogen) or 0.25 μg/ml human CYP2D6 (Invitrogen) in PBS overnight at 4°C and were then blocked with 10% FCS in RPMI 1640 for 2 h at room temperature. Total splenocytes diluted in DMEM containing 10% FCS were added in triplicates and incubated for 5 h at 37°C in 5% CO_2. Biotinylated goat anti–mouse IgG (1:1,000; SouthernBiotech) was added and plates were incubated overnight at 4°C. Horseradish peroxidase–conjugated Avidin D (1:1,000; Sigma-Aldrich) was added for 60 min at room temperature, and the reaction was developed by the addition of 3-amino-9-ethylcarbazole (Sigma-Aldrich).

Epitope mapping. Arrays of 162 staggered 12-mer synthetic peptides covering the entire human CYP2D6 sequence were covalently linked to nylon membranes (custom SPOTs service; Sigma-Aldrich). The N-terminal aa of the 12-mer peptides were shifted within the human CYP2D6 by three aa residues. Membranes were blocked for 6 h at room temperature in 2% dry milk/PBS before they were incubated overnight at 4°C in serum diluted 1:200 in wash buffer (blocking buffer containing 0.1% Tween 20). Membranes were washed four times in wash buffer and were then incubated at room temperature for 2 h with IRDye800-labeled secondary antibody (Rockland Immunochemicals, Inc.) diluted 1:20,000 in wash buffer. After two washes in wash buffer and three washes in PBS, fluorescence intensity was analyzed using an infrared imaging system (Odyssey; LI-COR Biosciences GmbH).

U. Christen is a Liver Fellow of the American Liver Foundation. This work is supported by National Institutes of Health grant R21 DK071577 (to U. Christen).

The authors declare that they have no competing financial interests.

Submitted: 29 August 2007
Accepted: 21 April 2008

REFERENCES

1. Limmer, A., J. Ohl, C. Kurts, H.G. Ljunggren, Y. Reiss, M. Groettrup, F. Momburg, B. Arnold, and P.A. Knolle. 2000. Efficient presentation of exogenous antigen by liver endothelial cells to CD8+ T cells results in antigen-specific T-cell tolerance. *Nat. Med.* 6:1348–1354.
2. Crispe, I.N. 2003. Hepatic T cells and liver tolerance. *Nat. Rev. Immunol.* 3:51–62.
3. Bowen, D.G., M. Zen, L. Holz, T. Davis, G.W. McCaughan, and P. Bertolino. 2004. The site of primary T cell activation is a determinant of the balance between intrahepatic tolerance and immunity. *J. Clin. Invest.* 114:701–712.
4. Chen, C.H., L.M. Kuo, Y. Chang, W. Wu, C. Goldbach, M.A. Ross, D.B. Stolz, L. Chen, J.J. Fung, L. Lu, and S. Qian. 2006. In vivo immune modulatory activity of hepatic stellate cells in mice. *Hepatology.* 44:1171–1181.
5. Alvarez, F., P.A. Berg, F.B. Bianchi, L. Bianchi, A.K. Burroughs, E.L. Cancado, R.W. Chapman, W.G. Cooksley, A.J. Czaja, V.J. Desmet, et al. 1999. International Autoimmune Hepatitis Group Report: review of criteria for diagnosis of autoimmune hepatitis. *J. Hepatol.* 31:929–938.
6. Krawitt, E.L. 2006. Autoimmune hepatitis. *N. Engl. J. Med.* 354: 54–66.
7. Manns, M.P., and A. Vogel. 2006. Autoimmune hepatitis, from mechanisms to therapy. *Hepatology.* 43:S132–S144.
8. Christen, U., and M.G. Herrath. 2004. Initiation of autoimmunity. *Curr. Opin. Immunol.* 16:759–767.
9. Manns, M.P., E.F. Johnson, K.J. Griffin, E.M. Tan, and K.F. Sullivan. 1989. Major antigen of liver kidney microsomal autoantibodies in idiopathic autoimmune hepatitis is cytochrome P450db1. *J. Clin. Invest.* 83:1066–1072.
10. Zanger, U.M., H.P. Hauri, J. Loeper, J.C. Homberg, and U.A. Meyer. 1988. Antibodies against human cytochrome P-450db1 in autoimmune hepatitis type II. *Proc. Natl. Acad. Sci. USA.* 85:8256–8260.
11. Zachou, K., E. Rigopoulou, and G.N. Dalekos. 2004. Autoantibodies and autoantigens in autoimmune hepatitis: important tools in clinical practice and to study pathogenesis of the disease. *J. Autoimmune Dis.* 1:2.
12. Oldstone, M.B.A. 1987. Molecular mimicry and autoimmune disease. *Cell.* 50:819–820.
13. Rose, N.R., and I.R. Mackay. 2000. Molecular mimicry: a critical look at exemplary instances in human diseases. *Cell. Mol. Life Sci.* 57:542–551.
14. Oldstone, M.B. 1998. Molecular mimicry and immune-mediated diseases. *FASEB J.* 12:1255–1265.
15. Christen, U., K.H. Edelmann, D.B. McGavern, T. Wolfe, B. Coon, M.K. Teague, S.D. Miller, M.B. Oldstone, and M.G. von Herrath. 2004. A viral epitope that mimics a self antigen can accelerate but not initiate autoimmune diabetes. *J. Clin. Invest.* 114:1290–1298.
16. Croxford, J.L., H.A. Anger, and S.D. Miller. 2005. Viral delivery of an epitope from *Haemophilus influenzae* induces central nervous system autoimmune disease by molecular mimicry. *J. Immunol.* 174:907–917.

17. Christen, U., and M.G. von Herrath. 2004. Induction, acceleration or prevention of autoimmunity by molecular mimicry. *Mol. Immunol.* 40:1113–1120.
18. Marceau, G., P. Lapierre, K. Beland, H. Soudeyns, and F. Alvarez. 2005. LKM1 autoantibodies in chronic hepatitis C infection: a case of molecular mimicry? *Hepatology.* 42:675–682.
19. Kammer, A.R., S.H. van der Burg, B. Grabscheid, I.P. Hunziker, K.M. Kwappenberg, J. Reichen, C.J. Melief, and A. Cerny. 1999. Molecular mimicry of human cytochrome P450 by hepatitis C virus at the level of cytotoxic T cell recognition. *J. Exp. Med.* 190:169–176.
20. Dalekos, G.N., P. Obermayer-Straub, M. Bartels, T. Maeda, A. Kayser, S. Braun, S. Loges, E. Schmidt, M.E. Gershwin, and M.P. Manns. 2003. Cytochrome P450 2A6: a new hepatic autoantigen in patients with chronic hepatitis C virus infection. *J. Hepatol.* 39:800–806.
21. Kerkar, N., K. Choudhuri, Y. Ma, A. Mahmoud, D.P. Bogdanos, L. Muratori, F. Bianchi, R. Williams, G. Mieli-Vergani, and D. Vergani. 2003. Cytochrome P4502D6(193-212): a new immunodominant epitope and target of virus/self cross-reactivity in liver kidney microsomal autoantibody type 1-positive liver disease. *J. Immunol.* 170:1481–1489.
22. Manns, M.P., K.J. Griffin, K.F. Sullivan, and E.F. Johnson. 1991. LKM-1 autoantibodies recognize a short linear sequence in P450IID6, a cytochrome P-450 monooxygenase. *J. Clin. Invest.* 88:1370–1378.
23. Oldstone, M.B.A., M. Nerenberg, P. Southern, J. Price, and H. Lewicki. 1991. Virus infection triggers insulin-dependent diabetes mellitus in a transgenic model: role of anti-self (virus) immune response. *Cell.* 65:319–331.
24. Lo, D., J. Freedman, S. Hesse, R.D. Palmiter, R.L. Brinster, and L.A. Sherman. 1992. Peripheral tolerance to an islet cell-specific hemagglutinin transgene affects both CD4+ and CD8+ T cells. *Eur. J. Immunol.* 22:1013–1022.
25. Corchero, J., C.P. Granvil, T.E. Akiyama, G.P. Hayhurst, S. Pimprale, L. Feigenbaum, J.R. Idle, and F.J. Gonzalez. 2001. The CYP2D6 humanized mouse: effect of the human CYP2D6 transgene and HNF4alpha on the disposition of debrisoquine in the mouse. *Mol. Pharmacol.* 60:1260–1267.
26. Yamamoto, A.M., D. Cresteil, O. Boniface, F.F. Clerc, and F. Alvarez. 1993. Identification and analysis of cytochrome P450IID6 antigenic sites recognized by anti-liver-kidney microsome type-1 antibodies (LKM1). *Eur. J. Immunol.* 23:1105–1111.
27. Kitazawa, E., T. Igarashi, N. Kawaguchi, H. Matsushima, Y. Kawashima, R.W. Hankins, and H. Miyakawa. 2001. Differences in anti-LKM-1 autoantibody immunoreactivity to CYP2D6 antigenic sites between hepatitis C virus-negative and -positive patients. *J. Autoimmun.* 17:243–249.
28. Gueguen, M., O. Boniface, O. Bernard, F. Clerc, T. Cartwright, and F. Alvarez. 1991. Identification of the main epitope on human cytochrome P450 IID6 recognized by anti-liver kidney microsome antibody. *J. Autoimmun.* 4:607–615.
29. Mehal, W.Z., A.E. Juedes, and I.N. Crispe. 1999. Selective retention of activated CD8+ T cells by the normal liver. *J. Immunol.* 163:3202–3210.
30. Reinhardt, R.L., A. Khoruts, R. Merica, T. Zell, and M.K. Jenkins. 2001. Visualizing the generation of memory CD4 T cells in the whole body. *Nature.* 410:101–105.
31. Ichiki, Y., S. Shimoda, H. Ishibashi, and M.E. Gershwin. 2004. Is primary biliary cirrhosis a model autoimmune disease? *Autoimmun. Rev.* 3:331–336.
32. Gut, J., U. Christen, and J. Huwyler. 1993. Mechanisms of halothane toxicity: novel insights. *Pharmacol. Ther.* 58:133–155.
33. Calne, R.Y., R.A. Sells, J.R. Pena, D.R. Davis, P.R. Millard, B.M. Herbertson, R.M. Binns, and D.A. Davies. 1969. Induction of immunological tolerance by porcine liver allografts. *Nature.* 223:472–476.
34. Ando, K., L.G. Guidotti, S. Wirth, T. Ishikawa, G. Missale, T. Moriyama, R.D. Schreiber, H.J. Schlicht, S.N. Huang, and F.V. Chisari. 1994. Class I-restricted cytotoxic T lymphocytes are directly cytopathic for their target cells in vivo. *J. Immunol.* 152:3245–3253.
35. Franco, A., L.G. Guidotti, M.V. Hobbs, V. Pasquetto, and F.V. Chisari. 1997. Pathogenetic effector function of CD4-positive T helper 1 cells in hepatitis B virus transgenic mice. *J. Immunol.* 159:2001–2008.
36. Moriyama, T., S. Guilhot, K. Klopchin, B. Moss, C.A. Pinkert, R.D. Palmiter, R.L. Brinster, O. Kanagawa, and F.V. Chisari. 1990. Immunobiology and pathogenesis of hepatocellular injury in hepatitis B virus transgenic mice. *Science.* 248:361–364.
37. Limmer, A., T. Sacher, J. Alferink, M. Kretschmar, G. Schonrich, T. Nichterlein, B. Arnold, and G.J. Hammerling. 1998. Failure to induce organ-specific autoimmunity by breaking of tolerance: importance of the microenvironment. *Eur. J. Immunol.* 28:2395–2406.
38. Voehringer, D., C. Blaser, A.B. Grawitz, F.V. Chisari, K. Buerki, and H. Pircher. 2000. Break of T cell ignorance to a viral antigen in the liver induces hepatitis. *J. Immunol.* 165:2415–2422.
39. Djilali-Saiah, I., P. Lapierre, S. Vittozi, and F. Alvarez. 2002. DNA vaccination breaks tolerance for a neo-self antigen in liver: a transgenic murine model of autoimmune hepatitis. *J. Immunol.* 169:4889–4896.
40. Derkow, K., C. Loddenkemper, J. Mintern, N. Kruse, K. Klugewitz, T. Berg, B. Wiedenmann, H.L. Ploegh, and E. Schott. 2007. Differential priming of CD8 and CD4 T-cells in animal models of autoimmune hepatitis and cholangitis. *Hepatology.* 46:1155–1165.
41. Lapierre, P., I. Djilali-Saiah, S. Vitozzi, and F. Alvarez. 2004. A murine model of type 2 autoimmune hepatitis: Xenoimmunization with human antigens. *Hepatology.* 39:1066–1074.
42. Welsh, R.M., and R.S. Fujinami. 2007. Pathogenic epitopes, heterologous immunity and vaccine design. *Nat. Rev. Microbiol.* 5:555–563.
43. Christen, U., and M.G. von Herrath. 2005. Infections and autoimmunity–good or bad? *J. Immunol.* 174:7481–7486.
44. Christen, U., D. Benke, T. Wolfe, E. Rodrigo, A. Rhode, A.C. Hughes, M.B. Oldstone, and M.G. von Herrath. 2004. Cure of prediabetic mice by viral infections involves lymphocyte recruitment along an IP-10 gradient. *J. Clin. Invest.* 113:74–84.
45. Zaccone, P., T. Raine, S. Sidobre, M. Kronenberg, P. Mastroeni, and A. Cooke. 2004. *Salmonella typhimurium* infection halts development of type 1 diabetes in NOD mice. *Eur. J. Immunol.* 34:3246–3256.
46. Selmi, C., and M.E. Gershwin. 2004. Bacteria and human autoimmunity: the case of primary biliary cirrhosis. *Curr. Opin. Rheumatol.* 16: 406–410.
47. Czaja, A.J. 2004. Autoimmune liver disease. *Curr. Opin. Gastroenterol.* 20:231–240.
48. von Herrath, M.G., R.S. Fujinami, and J.L. Whitton. 2003. Microorganisms and autoimmunity: making the barren field fertile. *Nat. Rev. Microbiol.* 1:151–157.
49. Czaja, A.J., and D.K. Freese. 2002. Diagnosis and treatment of autoimmune hepatitis. *Hepatology.* 36:479–497.
50. Lohr, H., M. Manns, A. Kyriatsoulis, A.W. Lohse, C. Trautwein, K.H. Meyer zum Buschenfelde, and B. Fleischer. 1991. Clonal analysis of liver-infiltrating T cells in patients with LKM-1 antibody-positive autoimmune chronic active hepatitis. *Clin. Exp. Immunol.* 84:297–302.
51. Lohr, H.F., J.F. Schlaak, A.W. Lohse, W.O. Bocher, M. Arenz, G. Gerken, and K.H. Meyer zum Buschenfelde. 1996. Autoreactive CD4+ LKM-specific and anticlonotypic T-cell responses in LKM-1 antibody-positive autoimmune hepatitis. *Hepatology.* 24:1416–1421.
52. Muruve, D.A., M.J. Barnes, I.E. Stillman, and T.A. Libermann. 1999. Adenoviral gene therapy leads to rapid induction of multiple chemokines and acute neutrophil-dependent hepatic injury in vivo. *Hum. Gene Ther.* 10:965–976.
53. Gonzalez, F.J., and A.M. Yu. 2006. Cytochrome P450 and xenobiotic receptor humanized mice. *Annu. Rev. Pharmacol. Toxicol.* 46:41–64.
54. Lenzi, M., G. Ballardini, M. Fusconi, F. Cassani, L. Selleri, U. Volta, D. Zauli, and F.B. Bianchi. 1990. Type 2 autoimmune hepatitis and hepatitis C virus infection. *Lancet.* 335:258–259.
55. Miyakawa, H., E. Kitazawa, K. Kikuchi, H. Fujikawa, N. Kawaguchi, K. Abe, M. Matsushita, H. Matsushima, T. Igarashi, R.W. Hankins, and M. Kako. 2000. Immunoreactivity to various human cytochrome P450 proteins of sera from patients with autoimmune hepatitis, chronic hepatitis B, and chronic hepatitis C. *Autoimmunity.* 33:23–32.
56. Michel, G., A. Ritter, G. Gerken, K.H. Meyer zum Buschenfelde, R. Decker, and M.P. Manns. 1992. Anti-GOR and hepatitis C virus in autoimmune liver diseases. *Lancet.* 339:267–269.
57. Lunel, F., N. Abuaf, L. Frangeul, P. Grippon, M. Perrin, Y. Le Coz, D. Valla, E. Borotto, A.M. Yamamoto, J.M. Huraux, et al. 1992. Liver/kidney microsome antibody type 1 and hepatitis C virus infection. *Hepatology.* 16:630–636.

58. Sugimura, T., P. Obermayer-Straub, A. Kayser, S. Braun, S. Loges, B. Alex, B. Luttig, E.F. Johnson, M.P. Manns, and C.P. Strassburg. 2002. A major CYP2D6 autoepitope in autoimmune hepatitis type 2 and chronic hepatitis C is a three-dimensional structure homologous to other cytochrome P450 autoantigens. *Autoimmunity*. 35:501–513.
59. Klein, R., U.M. Zanger, T. Berg, U. Hopf, and P.A. Berg. 1999. Overlapping but distinct specificities of anti-liver-kidney microsome antibodies in autoimmune hepatitis type II and hepatitis C revealed by recombinant native CYP2D6 and novel peptide epitopes. *Clin. Exp. Immunol.* 118:290–297.
60. Imaoka, S., N. Obata, T. Hiroi, M. Osada-Oka, R. Hara, S. Nishiguchi, and Y. Funae. 2005. A new epitope of CYP2D6 recognized by liver kidney microsomal autoantibody from Japanese patients with autoimmune hepatitis. *Biol. Pharm. Bull.* 28:2240–2243.
61. Longhi, M.S., M.J. Hussain, D.P. Bogdanos, A. Quaglia, G. Mieli-Vergani, Y. Ma, and D. Vergani. 2007. Cytochrome P450IID6-specific CD8 T cell immune responses mirror disease activity in autoimmune hepatitis type 2. *Hepatology*. 46:472–484.
62. Fairweather, D., and N.R. Rose. 2007. Coxsackievirus-induced myocarditis in mice: a model of autoimmune disease for studying immunotoxicity. *Methods*. 41:118–122.
63. Chartier, C., E. Degryse, M. Gantzer, A. Dieterle, A. Pavirani, and M. Mehtali. 1996. Efficient generation of recombinant adenovirus vectors by homologous recombination in *Escherichia coli*. *J. Virol.* 70:4805–4810.
64. Manns, M., G. Gerken, A. Kyriatsoulis, M. Staritz, and K.H. Meyer zum Buschenfelde. 1987. Characterisation of a new subgroup of autoimmune chronic active hepatitis by autoantibodies against a soluble liver antigen. *Lancet*. 1:292–294.